High-Order Sliding Mode Control of a Marine Current Turbine Driven Permanent Magnet Synchronous Generator

S.E. Ben Elghali[1], M.E.H. Benbouzid[1], J.F. Charpentier[2], T. Ahmed-Ali[3] and I. Munteanu[4]
[1]University of Brest, EA 4325 LBMS – IUT of Brest – Rue de Kergoat – CS 93837, 29238 Brest Cedex 03, France – E-mail: m.benbouzid@ieee.org
[2]French Naval Academy, EA 3634 IRENAV – Lanveoc-Poulmic, BP 600, 29240 Brest Armées, France
[3]University of Caen, UMR CNRS 6072 GREYC – Campus Côte de Nacre, Boulevard du Maréchal Juin, BP 5186, 14032 Caen Cedex, France
[4]Grenoble Polytechnic Institute, UMR CNRS 5269 G2ELAB – ENSE3, BP 46, 38402, Saint-Martin d'Hères, France

***Abstract*—This paper deals with the speed control of a Permanent Magnet Synchronous Generator (PMSG)-based Marine Current Turbine (MCT). Indeed, to increase the generated power and therefore the efficiency of an MCT, a nonlinear controller has been proposed. PMSG has been already considered for similar applications particularly wind turbine systems using mainly PI controllers. However, such kinds of controllers do not adequately handle some of tidal resource characteristics such as turbulence and swell effects. Indeed, these may decrease the MCT performances. Moreover, PMSG parameter variations should be accounted for. Therefore, a robust nonlinear control strategy, namely high-order sliding mode control, is proposed. The proposed control strategy is inserted in a global simulation tool that accounts for the resource and the marine turbine models. Simulations using tidal current data from the Raz de Sein (Brittany, France), and experiments on a 7.5-kW real-time simulator are carried out for validation purposes.**

***Index Terms*—Marine current turbine, Permanent magnet synchronous generator, modeling, nonlinear control, high-order sliding mode.**

NOMENCLATURE

PMSG	=	Permanent Magnet Synchronous Generator;
MCT	=	Marine Current Turbine;
HOSM	=	High-Order Sliding Mode;
ρ	=	Fluid density;
A	=	Cross-sectional area of the marine turbine;
V_{tide}	=	Fluid speed;
C_p	=	Power coefficient;
C	=	Tide coefficient;
V_{st} (V_{nt})	=	Spring (neap) tide current speed;
s, (r)	=	Stator (rotor) index;
d, q	=	Synchronous reference frame index;
V (I)	=	Voltage (Current);
P (Q)	=	Active (Reactive) power;
ϕ	=	Flux;
ϕ_f	=	Permanent magnet flux;
T_{em} (T_m)	=	Electromagnetic torque (Mechanical torque);
R	=	Resistance;
L	=	Inductance;
ω	=	Electrical angular speed;
f	=	Viscosity coefficient;
J	=	Turbine rotor inertia;
p	=	Pole pair number.

This work is supported by Brest Métropole Océane (BMO) and the European Social Fund (ESF). It is also supported by the GDR SEEDS CNRS N°2994 under the Internal Project HYDROLE. It is done within the framework of the Marine Renewable Energy Commission of the Brittany Maritime Cluster (Pôle Mer Bretagne).

I. INTRODUCTION

There are basically two ways of generating electricity from marine and tidal currents: by building a tidal barrage across an estuary or a bay in high tide areas, or by extracting energy from free flowing water (tidal kinetic energy). Within the last few decades, developers have shifted towards technologies that capture tidally-driven coastal currents or tidal stream [1]. The astronomic nature of this resource makes it predictable, to within 98% accuracy for decades, and independent of prevailing weather conditions. This predictability is critical to a successful integration of renewable energy in the electrical grid [2]. It is therefore obvious that there is a need to quantify the potential to generating electricity from these various sites [3]. In this context, and in previous works, different control strategies of control mainly for Doubly-Fed Induction Generator- (DFIG) based marine current turbines have been tested to evaluate the generated power [4-6].

In this paper, and in order to be able to compare and choose the adequate technology, a robust nonlinear control of a PMSG-based marine current turbine is carried out [7]. The adopted control strategy, namely high-order sliding mode (HOSM), relies on the resource and the marine turbine models that were validated by experimental data [8]. Simulations, using tidal current data from the Raz de Sein (Brittany, France), and experiments on a 7.5-kW real-time simulator are carried out for validation purposes.

II. MARINE CURRENT TURBINE MODELING [8]

The global scheme for a grid-connected marine current turbine is given by Fig. 1.

A. The Resource Model

1) Resource Potential. The total kinetic power in a marine current turbine has a similar dependence to that of a wind turbine and is governed by the following equation [9].

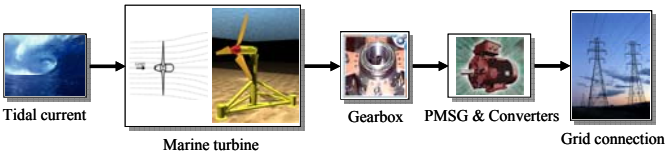

Fig. 1. Marine current turbine global block diagram.

$$P = \frac{1}{2}\rho A V_{tide}^3 \tag{1}$$

However, a marine energy turbine can only harness a fraction of this power due to losses and (1) is modified as follows.

$$P = \frac{1}{2}\rho C_p A V_{tide}^3 \tag{2}$$

For marine turbines, C_p is estimated to be in the range 0.35–0.5 [10].

2) Resource Model. Tidal current data are given by the SHOM (French Navy Hydrographic and Oceanographic Service) and is available for various locations in chart form. The SHOM available charts give, for a specific site, the current velocities for spring and neap tides. These values are given at hourly intervals starting at 6 hours before high waters and ending 6 hours after. Therefore, knowing tides coefficient, it is easy to derive a simple and practical model for tidal current speeds V_{tide}.

$$V_{tide} = V_{nt} + \frac{(C-45)(V_{st}-V_{nt})}{95-45} \tag{3}$$

Where 95 and 45 are respectively the spring and neap tide medium coefficient.

This first-order model is then used to calculate the tidal velocity each hour. The implemented model will allow the user to compute tidal velocities in a predefined time range. For illustration, Fig. 2 shows the model output for a month (March 2007). This adopted resource model has several advantages including its modularity not to mention its simplicity. Indeed, the marine turbine site can be changed, the useful current velocity can be adapted, and the time range taken into account can also be adapted from one month to one year.

B. The Turbine Rotor Model

The harnessing of the energy in a tidal flow requires the conversion of kinetic energy in a moving fluid, in this case water, into the motion of a mechanical system, which can then drive a generator.

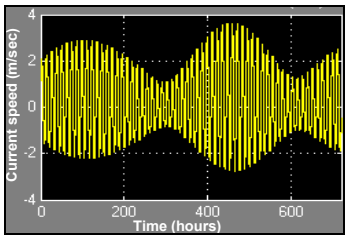

Fig. 2. Tidal velocity in the Raz de Sein for March 2007.

The harnessing of the energy in a tidal flow requires the conversion of kinetic energy in a moving fluid, in this case water, into the motion of a mechanical system, which can then drive a generator. It is not too surprising, therefore, that many developers suggest using technology that mirrors that which has been successfully utilized to harness the wind, which is also a moving fluid [1]. Moreover, much of the technology is based upon the use of horizontal axis turbines, such as that shown in Fig. 3. Therefore, much can be transferred from the modeling and operation of wind turbines. There are, however, a number of fundamental differences in the design and operation of marine turbines. Particular differences entail changes in force loadings, immersion depth, different stall characteristics, and the possible occurrence of cavitation [11].

The Blade Element Momentum (BEM) theory method has therefore been used for the marine turbine rotor modeling. Indeed, it is widely used in the industry as a computational tool to predict aerodynamic loads and power of turbine rotors [12]. It is relatively simple and computationally fast meeting the requirements of accuracy and control loop computational speed.

C. The PMSG Model

The generator chosen for the marine current system was the PMSG [13-15]. Indeed, the benefit of using a PMSG in renewable energy applications as an alternative to conventional generators is its higher efficiency. Moreover, the elimination of the gearbox and the introduction of variable speed control would further increase the availability of the system; reduce its active weight, and the need for maintenance. A schematic diagram of a PMSG-based generation system is shown in Fig. 4.

The PMSG dynamic equations are expressed in the *d-q* reference frame. The model of electrical dynamics in terms of voltage and current can be given as (4) [16]

$$\begin{cases} V_d = RI_d + L_d \dfrac{dI_d}{dt} - \omega L_q I_q \\ V_q = RI_q + L_q \dfrac{dI_q}{dt} + \omega L_q I_q - \omega \phi_f \end{cases} \tag{4}$$

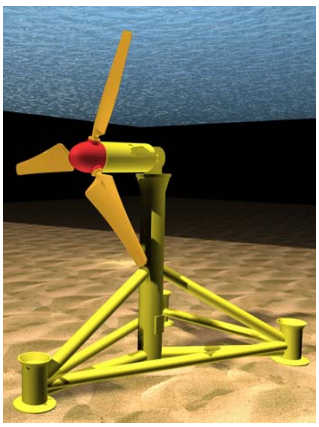

Fig. 3. Horizontal axis tidal turbine.

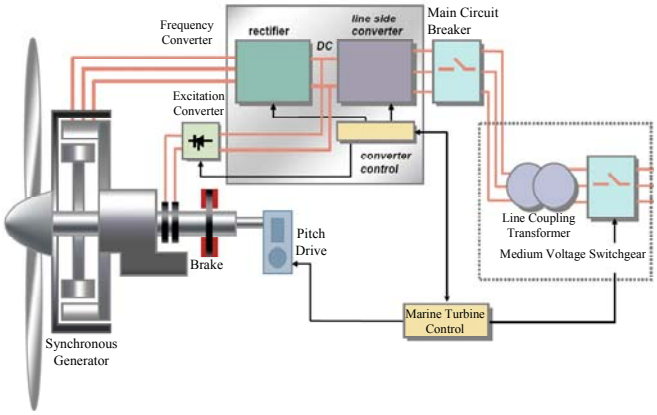

Fig. 4. Schematic diagram of a PMSG-based generation system.

The electromagnetic torque in the rotor is written as

$$T_{em} = \frac{3}{2} p\left[\left(L_d - L_q\right) I_d I_q - \phi_f I_q\right] \tag{5}$$

III. Control of the PMSG-Based Marine Current Turbine

A. Problem Formulation

A common practice in addressing PMSG control problem is to use a linearization approach [14], [16]. However, due to the tidal resource characteristics such as turbulence and swell effects and the inevitable uncertainties inherent in PMSG-based marine current turbines, such control methods come at the price of poor system performance and low reliability [17]. Hence the need for nonlinear and robust control to take into account these control problems. Although many modern techniques can be used for this purpose, sliding mode control has proved to be especially appropriate for nonlinear systems, presenting robust features with respect to system parameter uncertainties and external disturbances [18-21].

In particular, high-order sliding mode is especially appropriate to obtain simple control algorithms with extra features that are the elimination of the chattering phenomenon (main drawback of the traditional sliding mode approach) and a finite reaching time [22-23]. Up to now, a few second-order sliding mode control approaches have been introduced for wind and marine applications [4], [24-25].

B. Second-Order Sliding Mode Control Approach

As the chattering phenomenon is the major drawback of practical implementation of sliding mode control, the most efficient ways to cope with this problem is higher order sliding mode. This technique generalizes the basic sliding mode idea by acting on the higher order time derivatives of the sliding manifold, instead of influencing the first time derivative as it is the case in the standard (first order) sliding mode. This operational feature allows to completely mitigating the chattering effect, keeping the main properties of the original approach [24].

The proposed control strategy is based on a step-by-step procedure: First, the speed reference ω_{ref} is generated by a Maximum Power Point Tracking (MPPT) strategy [5]. Then, an optimal electromagnetic torque, which ensures the rotor speed convergence to ω_{ref} is computed using the following equation.

$$T_{em\_ref} = T_m + f\omega - \alpha(\omega - \omega_{ref}) + J\dot{\omega}_{ref} \tag{6}$$

where α is a positive constant. Afterwards, current references are derived to ensure the PMSG torque convergence to the optimal torque.

$$\begin{cases} I_{d\_ref} = 0 \\ I_{dr\_ref} = \dfrac{2}{3}\dfrac{T_{em}}{p\phi_f} \end{cases} \tag{7}$$

In order to ensure the currents convergence to their references, a second-order sliding mode strategy is used. Let us define the following sliding surfaces.

$$\begin{cases} S_1 = I_d - I_{d\_ref} \\ S_2 = I_q - I_{q\_ref} \end{cases} \tag{8}$$

It follows that

$$\begin{cases} \dot{S}_1 = \dot{I}_d - \dot{I}_{d\_ref} \\ \ddot{S}_1 = \varphi_1(t,x) + \gamma_1(t,x)V_d \end{cases} \tag{9}$$

and

$$\begin{cases} \dot{S}_2 = \dot{I}_q - \dot{I}_{q\_ref} \\ \ddot{S}_2 = \varphi_2(t,x) + \gamma_2(t,x)V_q \end{cases} \tag{10}$$

Where $\varphi_1(t,x)$, $\varphi_2(t,x)$, $\gamma_1(t,x)$, and $\gamma_2(t,x)$ are uncertain bounded functions that satisfy

$$\begin{cases} \varphi_1 > 0, \quad |\varphi_1| > \Phi_1, \quad 0 < \Gamma_{m1} < \gamma_1 < \Gamma_{M1} \\ \varphi_2 > 0, \quad |\varphi_2| > \Phi_2, \quad 0 < \Gamma_{m2} < \gamma_2 < \Gamma_{M2} \end{cases}$$

The proposed control approach has been designed using the supertwisting algorithm that has the additional advantage of only requiring information of the sliding variable, but not of its derivative [22]. The proposed second-order sliding mode controller contains two parts:

$$\begin{cases} V_d = u_1 + u_2 \\ V_q = w_1 + w_2 \end{cases} \tag{11}$$

where $\begin{cases} \dot{u}_1 = -\alpha_1 sign(S_1) \\ u_2 = -\beta_1 |S_1|^{\rho} sign(S_1) \end{cases}$ and $\begin{cases} \dot{w}_1 = -\alpha_2 sign(S_2) \\ w_2 = -\beta_2 |S_2|^{\rho} sign(S_2) \end{cases}$

In order to ensure the convergence of the sliding manifolds to zero in finite time, the gains can be chosen as follows [23].

$$\begin{cases} \alpha_i > \dfrac{\Phi_i}{\Gamma_{mi}} \\ \beta_i^{\,2} \geq \dfrac{4\Phi_i}{\Gamma_{mi}^{\,2}} \dfrac{\Gamma_{Mi}(\alpha_i + \Phi_i)}{\Gamma_{mi}(\alpha_i - \Phi_i)}; \quad i = 1,2 \\ 0 < \rho \leq 0.5 \end{cases}$$

The above proposed second-order sliding mode control strategy for a PMSG-based marine current turbine is illustrated by the block diagram in Fig. 5.

Finally and as an additional justification of such an advanced controller, it should be noted that its practical implementation implies an online computational cost similar to that of PI or PID controllers [24].

IV. Validation Results

A. Validation Using the Developed Simulation Tool

1) Validation Data and Parameters. In this work, the Raz de Sein site was chosen above several others listed in the European Commission report EUR16683 [34] due to the presence of high speed current coupled with appropriate depths suitable for marine turbine. Moreover, the marine current speed distribution for most of the time is greater than the minimum, estimated to be 1 m/sec, required for economic deployment of marine turbine.

The turbine rotor model was validated through the comparison of the simulation model with experimental data from the available literature [8] (Fig. 6). The adopted marine current turbine is of 1.44 m diameter rated at 7.5-kW. In this context, the obtained power coefficient C_p and the extractable power curves are shown by Fig. 7.

The 7.5-kW PMSG parameters are given in the appendix.

2) Simulations. In this case, the marine current turbine is simulated considering a resource first-order model (3). Therefore, for speed references given by Fig. 8 (MPPT) and a resource illustrated by Fig. 9, the PMSG-based MCT control performances are shown in Figs. 10, 11 and 12 respectively illustrating the current, the rotor speed, and the generated power.

The obtained results show good tracking performances of the PMSG current and rotor speed. Moreover, regarding [5] and as expected, the generated power is smoothest.

Fig. 6. The tested marine turbine [27].

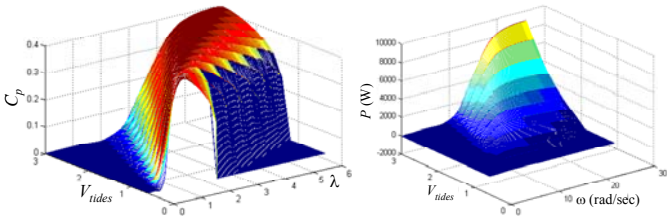

(a) $C_p(\lambda, V_{tides})$ curves. (b) The extractable power $P(\omega, V_{tides})$.

Fig. 7.

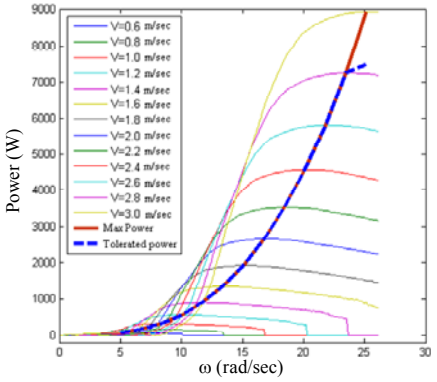

Fig. 8. Power curves for different tidal current speeds.

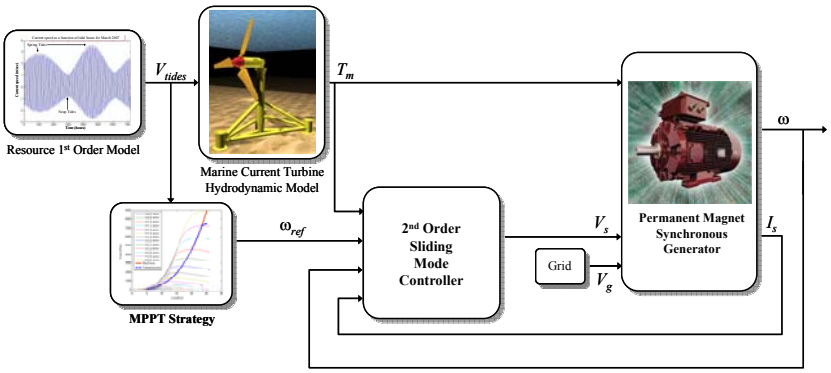

Fig. 5. The proposed control structure.

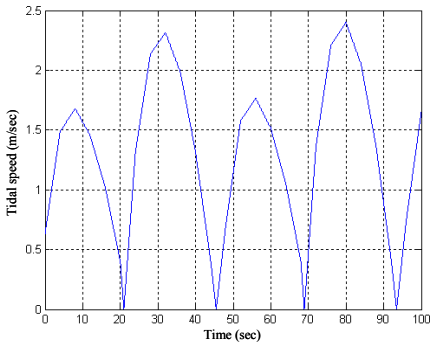

Fig. 9. The resource tidal speed.

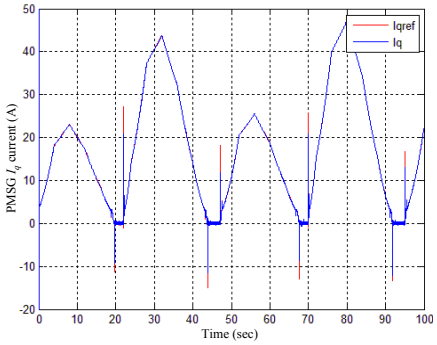

Fig. 10. The PMSG I_q current tracking performances.

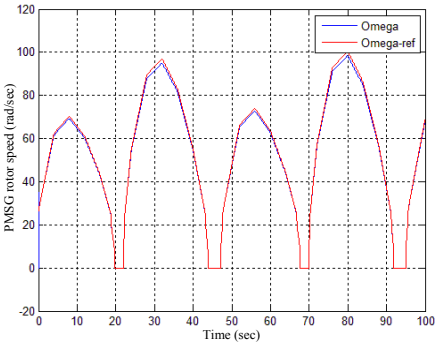

Fig. 11. The PMSG rotor speed tracking performances.

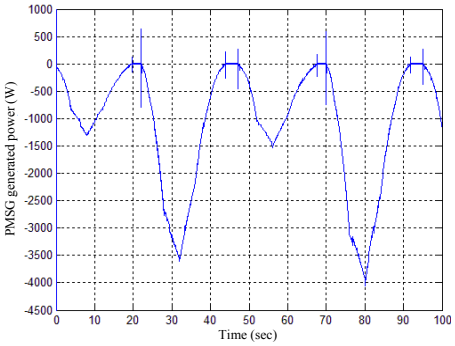

Fig. 12.The PMSG generated power.

B. Experimental Tests

For experimental validation of the proposed second-order sliding mode control approach, experiments where carried out using the Grenoble Institute of Technology, France (G2ELAB) renewable energy test bench.

1) The test bench [18]. The test bench presented in Fig. 13 allows the physical simulation of the marine power system. The MCT is emulated by a DC motor, which reproduces the torque and the inertia with respect to tidal speeds. The DC motor is coupled to a 7.5-kW PMSG (Appendix).

2) Experimental tests. The experimental tests where carried out to be as close as possible to the simulation conditions for the marine current turbine of Fig. 6. In these conditions, Figs. 14 to 15 show experimental control performances of the emulated PMSG-based MCT. These results, as in simulations, show very good tracking performances in terms of the PMSG current and rotor speed. Moreover, for comparison purposes, Fig. 16 shows simulation versus experimental results of the generated power. The obtained results are quite satisfactory as it is obvious that it is not possible to exactly emulate the marine turbine behavior. The test bench is equipped with current and torque limitations that explain some of Fig. 16 differences, in particular for high power generation. Moreover, the MCT hydrodynamic model uses torque limitations that justify a purely positive generated power in simulation [8].

V. CONCLUSIONS

This paper dealt with a second-order sliding mode control of PMSG-based marine current turbine. The proposed control strategy relies on the resource and the marine turbine models.

Fig. 13. Components of the G2ELAB test bench, Grenoble, France: ① DC motor, ② PMSG, ③ Power electronics for driving the DC motor, ④ Power electronics for driving the PMSG, ⑤ DSP TMS320F240 implementing DC motor control, ⑥ DSP DS1005 (dSPACE) implementing PMSG-based MCT control.

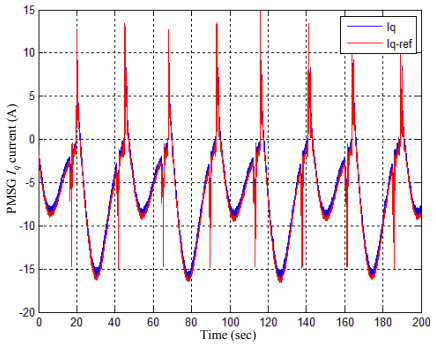

Fig. 14. Experimental PMSG I_q current tracking performances.

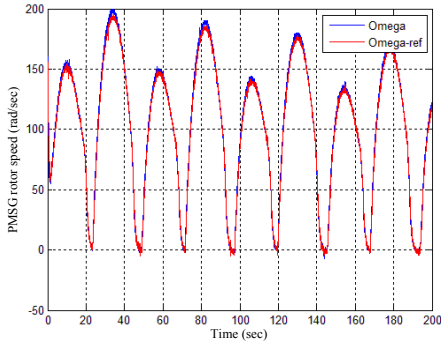

Fig. 15. Experimental PMSG rotor speed tracking performances.

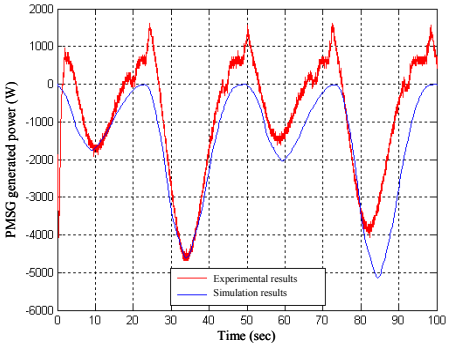

Fig. 16. Output power: Experimental vs simulation.

Its main features are a chattering-free behavior, a finite reaching time, and robustness with respect to external disturbances (e.g. grid) and unmodeled dynamics.

Tidal current data from the Raz de Sein (Brittany, France) have been used to run simulations of a 7.5-kW prototype over various flow regimes and experimental test have been carried out on a 7.5-kW PMSG test bench. The obtained results are satisfactory and very encouraging. Moreover, the experimental tests have shown that the practical implementation of the proposed second-order sliding mode controller implies an online computational cost similar to that of PI or PID controllers.

APPENDIX

PARAMETERS OF THE SIMULATED AND TESTED PMSG

$R = 0.173$ mΩ, $L_d = 0.085$ mH, $L_q = 0.951$ mH, $\phi_f = 0.112$ Wb
$J = 0.0048$ kg.m^2, $f = 8.5\ 10^{-3}$ Nms^{-1}

REFERENCES

[1] S.E. Ben Elghali et *al.*, "Marine tidal current electric power generation technology: State of the art and current status," *in Proceedings of IEEE IEMDC'07*, Antalya (Turkey), vol. 2, pp. 1407-1412, May 2007.

[2] *2005 IEEE Power Engineering Society General Meeting Panel Session*, "Harnessing the untapped energy potential of the oceans: Tidal, wave, currents and OTEC," San Francisco (USA), June 2005.

[3] L. Myers et *al.*, "Simulated electrical power potential harnessed by marine current turbine arrays in the Alderney Race," *Renewable Energy*, vol. 30, p. 1713-1731, 2005.

[4] S.E. Ben Elghali et *al.*, "High-order sliding mode control of DFIG-based marine current turbine", *in Proceedings of the IEEE IECON'08*, Orlando, Florida (USA), pp. 1228-1233, November 2008.

[5] S.E. Ben Elghali et *al.*, "Modeling and MPPT sensorless control of a DFIG-based marine current turbine," *in Proceedings of the ICEM'08*, Vilamoura (Portugal), September 2008.

[6] J.W. Park et *al.*, "Wide speed operation of a doubly-fed induction generator for tidal current energy," *in Proceedings of the IEEE IECON'04*, Busan (South Korea), vol. 2, pp. 1333-1338, November 2004.

[7] S.M. Abu Sharkh et *al.*, "Performance of an integrated water turbine pm generator," *in Proceedings of IEE PEMD'02*, vol. 2, pp. 486-491, Bath (UK), April 2002.

[8] S.E. Ben Elghali et *al.*, "A simulation model for the evaluation of the electrical power potential harnessed by a marine current turbine," *IEEE Journal on Oceanic Engineering*, vol. 32, n°4, pp. 786-797, October 2007.

[9] J.S. Couch et *al.*, "Tidal current energy extraction: Hydrodynamic resource characteristics," *Proc. IMechE*, Part M: *Journal of Engineering for the Maritime*, vol. 220, n°4, pp. 185-194, 2006.

[10] L. Myers et *al.*, "Power output performance characteristics of a horizontal axis marine current turbine," *Renewable Energy*, vol. 31, pp. 197-208, 2006.

[11] W.M.J. Batten et *al.*, "Hydrodynamics of marine current turbines," *Renewable Energy*, vol. 31, pp. 249-256, 2006.

[12] G. Mattarolo et *al.*, "Modelling and simulation techniques applied to marine current turbine," *in Proceedings of the 2006 International Conference on Ocean Energy*, Bremerhaven (Germany), 2006.

[13] J.F. Conroy et *al.*, "Frequency response capability of full converter wind turbine generators in comparison to conventional generation," *IEEE Trans. Power Systems*, vol. 23, n°2, pp. 649-656, May 2008.

[14] M. Chinchilla et *al.*, "Control of permanent-magnet generators applied to variable-speed wind-energy systems connected to the grid," *IEEE Trans. Energy Conversion*, vol. 21, n°1, pp. 130-135, March 2006.

[15] J.M. Carrasco et *al.*, "Power-electronic systems for the grid integration of renewable energy sources: A survey," *IEEE Trans. Industrial Electronics*, vol. 53, n°4, pp. 1002-1016, June 2006.

[16] K. Tan et *al.*, "Optimum control strategies in energy conversion of PMSG wind turbine system without mechanical sensors," *IEEE Trans. Energy Conversion*, vol. 19, n°2, pp. 392-399, June 2004.

[17] A. Mirecki et *al.*, "Architecture complexity and energy efficiency of small wind turbines," *IEEE Trans. Industrial Electronics*, vol. 54, n°1, pp. 660-670, February 2007.

[18] I. Munteanu et *al.*, "Energy-reliability optimization of wind energy conversion systems by sliding mode control," *IEEE Trans. Energy Conversion*, vol. 23, n°3, pp. 975-985, September 2008.

[19] B. Beltran et *al.*, "Sliding mode power control of variable-speed wind energy conversion systems," *IEEE Trans. Energy Conversion*, vol. 23, n°2, pp. 551-558, June 2008.

[20] J. Matas et *al.*, "Feedback linearization of direct-drive synchronous wind-turbines via a sliding mode approach," *IEEE Trans. Power Electronics*, vol. 23, n°3, pp. 1093-1103, May 2008.

[21] F. Valenciaga et *al.*, "Variable structure control of a wind energy conversion system based on a brushless doubly fed reluctance generator," *IEEE Trans. Energy Conversion*, vol. 22, n°2, pp. 499-506, June 2008.

[22] A. Levant et *al.*, "Integral high-order sliding modes," *IEEE Trans. Automatic Control*, vol. 52, n°7, pp. 1278-1282, July 2007.

[23] L. Fridman and A. Levant, *Sliding Mode Control in Engineering*, Marcel Dekker, Inc., 2002, Chap. 3 Higher Order Sliding Modes, pp. 53-101.

[24] F. Valenciaga et *al.*, "High-order sliding control for a wind energy conversion system based on a permanent magnet synchronous generator," *IEEE Trans. Energy Conversion*, vol. 23, n°3, pp. 860-867, September 2008.

[25] B. Beltran et *al.*, "High-order sliding mode control of variable speed wind turbines," *IEEE Trans. Industrial Electronics*, IEEE Xplore – 10.1109/TIE.2008.2006949, 2009.

[26] EU Commission, "The exploitation of tidal marine currents," *Report EUR16683EN*, 1996.

[27] A.S. Bahaj et *al.*, "Power and thrust measurements of marine current turbines under various hydrodynamic flow conditions in a cavitation tunnel and a towing tank," *Renewable Energy*, vol. 32, pp. 407-426, 2007.